

Link	Length	ID	OD
Shoulder Link	550mm	42mm	50mm
Elbow Link	400mm	42mm	50mm

Table 1: Dimensions of various links

### 3.6 Base Rotation

This part connects the robotic arm to the chassis of the rover with the motor and gearbox providing rotation of 330 deg to the entire arm. The base is designed based on a caging mechanism as shown in figure 14 to support the heavy loading and provide stability to the arm. The gearbox used is strain wave gear or commonly referred as harmonic drive.

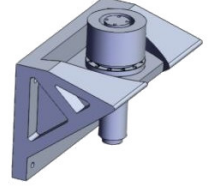


Figure 14: Base Rotation design

## 4 Bioassembly

“There is a theory which states that if ever anyone discovers exactly what the Universe is for and why it is here, it will instantly disappear and be replaced by something even more bizarre and inexplicable. There is another theory which states that this has already happened.”

### 4.1 Science Plan

#### Microscopic examination

Microscopes are optical-based instruments that magnify the small bacteria image [11]. Bacteria can directly be seen under microscope or it can be differentiated from each other using different stains such as safranin staining, Gram positive- negative staining, or acid-fast staining etc [12][13].

#### Gram staining test

The microscope can be used to observe live or dead cells. Since, it is difficult to convey the extinct or extant life other test can be performed in combination with it. Safranin dye is prepared in 95% ethanol for staining purpose. For analysis, a smear from the given soil solution is prepared on a clean glass slide. After drying the dye was added and incubated. After that the smear was washed, dried and observed under the microscope. The safranin dye colors the cell nuclei red, thus cells appear red colored when seen under microscope, as seen in figure 16a

#### XTT dye reduction test

In case of dormant life forms such as spores that can be grown with the use of nutrients and thus can also be detected using XTT dye. This could provide prelims evidence of life forms in extra-

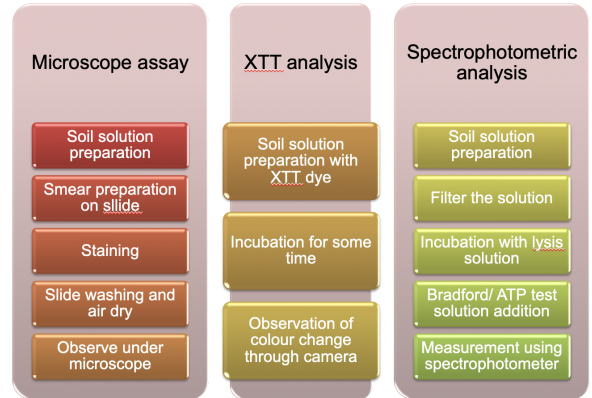
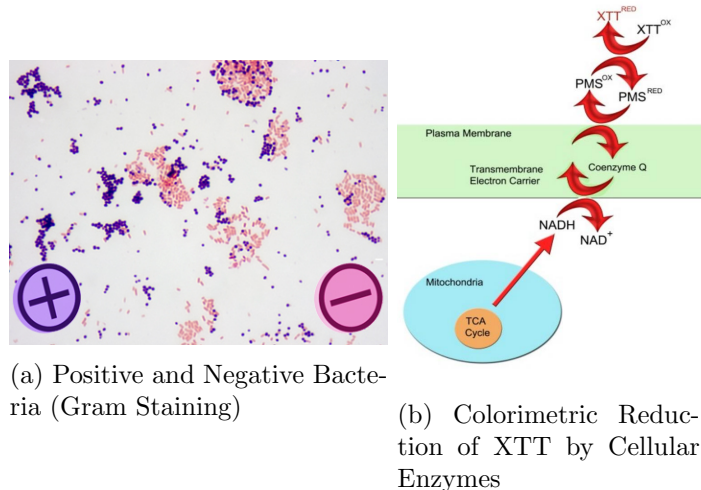


Figure 15: Science Plan

terrestrial locations. Living organisms have simultaneous transfer of electrons or proton within the cell require continuous energy source to carry out their metabolic functions like respiration, oxidative phosphorylation etc. These processes involve several redox molecules, as depicted in figure 16b. These processes can be exploited to detect the living cells. The result of colour change can be concluded with digital images, therefore it is one of the convenient onsite tests.[14]



## Spectroscopic method to Measure the organic molecules

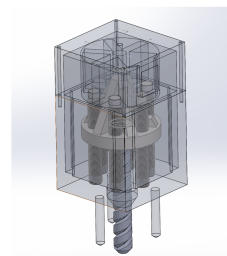
In life science laboratories, UV spectrophotometry is typically used for the analysis of protein, amino acid, DNA, RNA, ATP, carbohydrates and other cellular components [15]. These macromolecules are critical for the survival. Detection of the macromolecules using spectrophotometer gives indirect evidence for presence of life forms as they are mostly unstable in outside environment. [16]

### A. Bradford for protein test

This involves the use of Coomassie brilliant blue G-250 dye that forms a complex with the protein in solution.[17] Bradford is brown colour solution initially that changes to blue colour when complexed with protein. Upon presence of protein, change of colour is obtained that can be measured at 595 nm. The higher intensity of blue colour indicates the high protein concentration.[16]

### B. ATP test

Adenosine Triphosphate (ATP) is known as the energy currency in the living organisms. The energy released after catabolism of ATP drives most of the cellular processes [18]. The assay used for ATP measurement is based on the phosphorylation of glycerol in order to generate a product that is green in colour and can be easily quantified colorimetrically at OD 570 nm [19]. Higher the amount of ATP will have intensified colour.



## 4.2 Soil Sample Acquisition System: Design Overview

We have developed Hollow drill for purpose of soil sample acquisition, shown in figure 17, capable of drilling 100 mm deep. Drill Assembly will be attached to Robotic Arm, allowing better reachability of combined system such that difficult terrain topography doesn't limit scientific investigation.

Figure 17: Soil Sample Acquisition System

**Mass:** 9.97 Kg

**Materials:** Tungsten carbide, Al 7075, Ti-6 Al-4V

**Size of the drill:** 228mm (length)

**Total Size (mm):** 150x150x250

Rock Samples are collected with gripper of the robotic arm and transported to Microscope Assembly Module on the chassis consisting of 3 different inlets such that analysis of the rocks is done exclusively for each sample through Microscope and XTT dye test as well as other chemical tests on Stewart platform. Our Choice of the appropriate mechanism for drilling is based on ability to sample diverse soil types (such as solid rock, hard soil, porous/spongy soil), functionality and efficiency in harsh conditions. In order to prevent dust from entering, a shutter mechanism is utilized in the drill as an enclosure, as observed in figure 18.[20]

Choice of the Coring Drill (Hollow drill) instead of normal drill accounts for additional simplicity and robustness achieved in the sample distribution part. Transferring the sample directly to Test module inlets with the help of the Robotic Arm achieves better prevention of contamination than transferring through the channel system.

#### 4.2.1 Modeling and Simulations of Drill Based Sample Acquisition System

The first step followed for simulating the drilling mechanism was to find out how the drill will behave and work in the martian regolith and what kind of forces will be applied to it? To solve these problems we modeled the system utilizing Explicit Dynamics in ANSYS. Simulation results are shown in figure 20. Utilizing Data for Martian Simulant [21] and considering the average ambient temperature -63 degrees Celsius and gravity.

In the result, we obtained reaction forces on a drill which was 69N for tungsten carbide drill and additional deformation characteristics were obtained. Which was utilized for further analysis.

To establish structural reliability and to ensure the system works as intended Static Structural Analysis was performed in ANSYS with Forces obtained from Explicit Dynamics and applying gravity considerations. Simulation results shown in figure 19. In Conclusion, It's found structure is highly reliable due to 2 factors 1) Appropriate choice of material 2) Lack of large valued forces on the drill as per mission requirement which is to drill upto which is to 100mm. This led to further development and decision regarding other components.

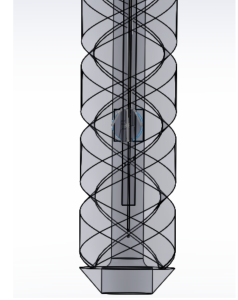


Figure 18: Coring Drill

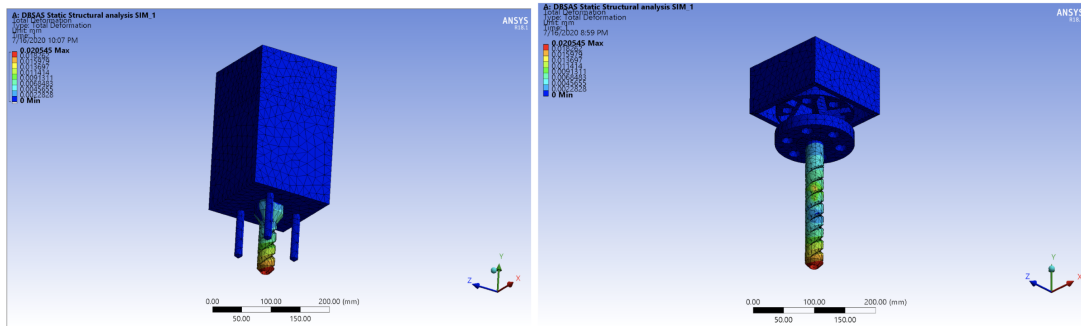


Figure 19: Impact Forces simulation results

	Power requirement	Torque requirement
<b>Drill Motor</b>	<b>116 W</b>	<b>23 mNm</b>
<b>Motor for feed (Screw drive)</b>	<b>45 W</b>	<b>40 mNm (raise) and 32 mNm (feed)</b>

Table 2: Motor requirements

It was found from research by Robin Phillips under ESA development contract that The COTS motors RE13 and EC22 are capable of standing up to the launch vibration and shock and a landing on Mars and then functioning for the full planned ExoMars mission in the environmental conditions found on Mars. [22]

After performing simulations on the structure and as per design requirement choice of motor and its specifications was made, Calculation of Motor power and torque requirement was done applying Mechanical basic drilling formulas[23]. Results are tabulated in table 2 Ultimately the actuator warm-up heaters will play an active role in maximizing the utility and science return of the rover. We will be using a Kapton film heater which was also implemented by NASA in previous Mars rover missions, after analysis it was concluded to be the best option considering the simplicity and application to reckon it also presents trade off in terms of energy utilization and complication in the electrical part.[24]

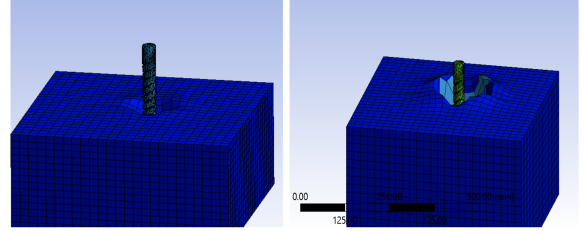


Figure 20: Reaction Forces simulation results

#### 4.2.2 Thermal analysis

The thermal analysis of the drill is necessary to prevent issues such as the burning of the drill bit at high-temperature, modification of sampled content, and loss of scientific validity due to the heat generated by the dry drilling process. The thermal analysis was done using the fast numerical method proposed by Jinsheng et. al.[25] The thermal problem was viewed as a one dimensional transient heat transfer problem in a semi-infinite object. The simplified drill was modeled using a heat conduction differential equation and a fast numerical calculation method, with time and the drill discretized. The model was modified to consider the effects of radiation, and drill bit configuration without convection.

The equivalent heat flow into the drill is given by  $q_e = k_e \cdot (\text{Power of drill})$  where the correction coefficient( $k_e$ ) accounts for the heat generated, the heat partition between the drill and martian soil, and the 1D model simplification. It has to be experimentally determined, but in this analysis, we took it to be 1, i.e.,  $k_e=1$ , which gives us the upper limit of the drill's temperature distribution. Also, during drilling, the torque and angular speed vary, so the maximum of there parameter is taken to account for the highest heat flow in the drill that may occur. The conditions, as mentioned above, help us ensure that we design the drill to withstand the most elevated temperatures that we might encounter.

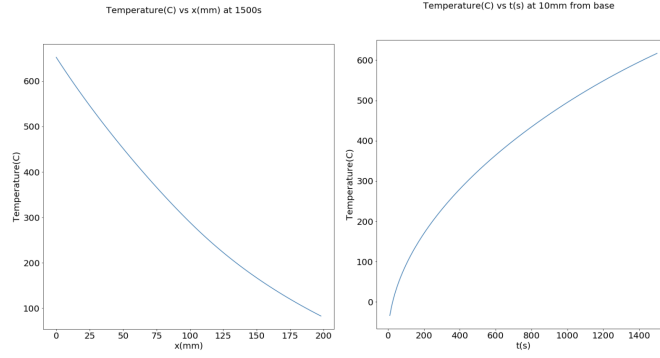


Figure 21: Drilling depth 100mm

### 4.3 Microscopy Assembly

#### 4.3.1 Setup

Setup to observe microbial presence in the soil sample solution with water medium, placed on a glass slide using tube channeling from central soil solution beaker, is an assembly of a 6 DOF parallel manipulator (stewart platform) fixed to a square platform with a vertical stand of 472 mm height suspending circular array of syringes filled with required chemicals and a Dino-Lite 1000X microscope.[26]

Microscope, array of syringes and soil solution tube are placed at one level, while linear actuator for pressing syringe's piston and servo motor to position the actuator over syringes sequentially in accordance to science plan for testing is placed at a higher level on the vertical stand. Stewart platform is used to mimic motion of slide. CAD assembly is shown in figure 22

#### 4.3.2 Material and Manufacturing

Overall dimensions of the setup is base area of 220x220 sq-mm and height 520 mm. Entire setup is enclosed within a temperature controlled box. The main microscopy assembly is designed to operate in temperature range of 20-30° C. Materials for various parts are selected in accordance with static structural, thermal simulations and manufacturability ease and accuracy. Vertical stand and square base are of Aluminium Alloy while microscope holder and linear actuator positioner are made up of TPU Stewart platform has base and platform made up of acrylic sheet shaped using laser cutting, and supporting rods are of stainless steel with threading at the ends for stainless steel female rod end bearings.

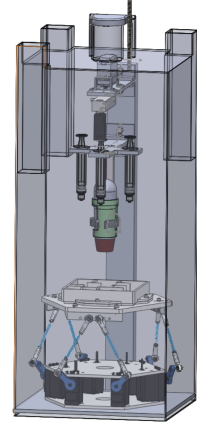


Figure 22: Microscopy Assembly

#### 4.3.3 Stewart Platform

A fairly precise stewart platform with six degrees of freedom is built that takes input of the translation vector and three euler angles and finally directing the servos to move accordingly, shown in figure 23b The platform has 6 degrees of freedom with respect to base frame- 3 translational and 3 angular. Further discussed in Appendix 11.4.

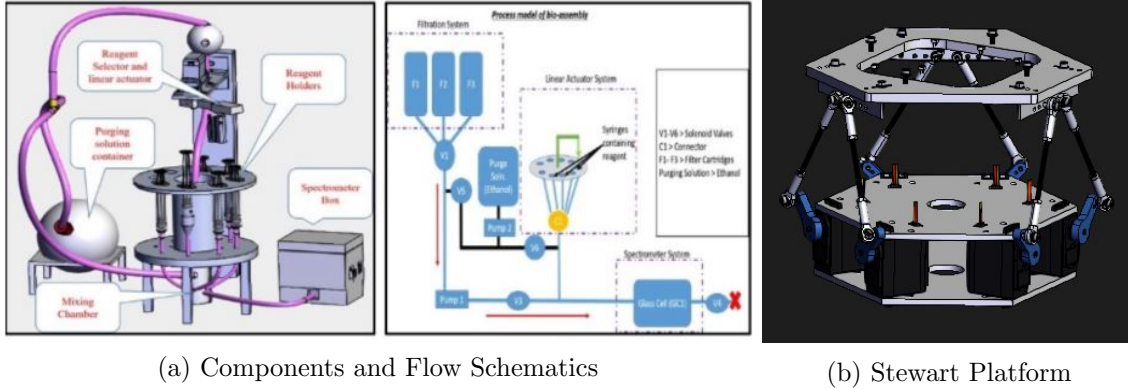


Figure 23

#### 4.4 Spectrophotometer and Chemical Reactor Assembly

The problem statement of the IRDC requires the detection of life and its classification as extinct or extant. To serve this purpose, we are proposing a number of tests to be conducted on rover. Among these tests, some tests will be performed using a spectroscopy assisted detection system namely called as the spectrometer assembly. Flow schematics are shown in figure 23a.

Throughout the last decade, portable spectrometers have become more useful in case of field analysis of contaminants or in soil analysis.[27][28][29] The main drawbacks of using conventional spectrometers mainly comprises of its huge power requirements and vibration susceptibility of precision optics in it. For these reasons LED spectrometers have become more pertinent in this field through the last decade. Keeping this idea in mind, we have also incorporated indigenously developed spectrometer assembly which also uses LEDs as light source and light dependent resistor (LDR) as detector. We are proposing the use of this module to quantify the amount protein and NPK content present in the soil sample with the help of colorimetric detection techniques.

##### 4.4.1 Assembly Overview and Analysis

The whole assembly system needs to be protected from the absolute temperature difference occurring on the surface of Mars. For this reason, we have enclosed the whole system inside a thermally controlled enclosed environment, discussed in 11.4.

We have conducted computational fluid dynamics simulations. The CFD models (2D) are designed with the same materials property and dimensions as our designed 3D model has. The simulation studies were performed using ANSYS Fluent CFD simulation environment on K-epsilon Viscous Model. The initial simulations indicate a good flow inside the fluid channels without flow separation. We also tested for different type of fluids in which the results are satisfactory in terms of flow parameters. Simulation results to be found in appendix 11.4.

## 5 Chassis

The chassis is made of AA7075 - T6 structural members. The cross section of the structural members is 20mm x 20mm x 2mm, resulting in a total weight of 8.187 kg. We incorporated stiffeners, gussets, and other supporting elements as seen in figure 24 to support assemblies which applied high force and moments locally. These were added after analyzing the static structural

where:

$P_{cr}$  - maximum load

$F_c$  = end fixity factor (this is 0.25 for one end fixed, one end free; 1.0 for both ends supported; 2.0 for one end fixed, one end simple; and 4.0 for both ends rigid)

$d$  = root diameter of screw; and

$L$  = the distance between the nut and load-carrying bearing.

All screw mechanisms have a critical velocity — the rotational velocity limit of the screw after which vibrations develop due to the shaft's natural harmonic frequency. This is also commonly called “screw whip” and depends on the diameter and length of the screw between supports.

$$N = \frac{4.76 \times 10^6 \times d \times F_c}{L^2} \quad (17)$$

where:

$N$  = critical speed,

$d$  = root diameter of screw,

$F_c$  is end fixity factor (this is 0.36 for one end rigidly fixed, one end free; 1.00 for both ends supported; 1.47 for one end rigidly fixed, one end supported; and 2.23 for both ends rigidly fixed)

$L$  = the length between bearing supports.

## 11.4 Bioassembly

### 11.4.1 Combining microscopic, XTT dye test and spectroscopic tests

The combined results from all tests can be used to analyze extinct and extant life in extraterrestrial locations. These can be done as follows:

- When microscope shows the presence of microbes, XTT dye test and spectroscopy results also shows colour change, then that can be concluded as the presence of extant life as these changes can be done by viable cells.
- When microscope shows the presence of microbes, XTT and spectroscopy tests shows no colour change, then it can be concluded as extinct life. As safranin stain can enter the dead cells and that can be observed under microscope.
- When microscope shows the absence of microbes and XTT and spectroscopy tests also shows no colour change, this can be concluded as the absence of life forms.
- Lastly, when microscope shows absence of microbes and XTT and spectroscopy tests shows colour change, this can be concluded as extant life as spores might be present in the given sample that is difficult to be observed under microscope

### 11.4.2 Material Selection

The temperature on Mars varies on average from -63°C to a maximum temperature of about 25°C and a minimum recorded temperature of -140°C. Typical operational temperature range of mechanical instruments on Mars is in a range of -70°C to 45°C. The instrument can also operate at a lower temperature, providing that the critical components (e.g. actuators, gears, lubricants) are heated to the minimum operational temperature.

Apart from Thermal conditions, On present-day Mars, the total integrated UV flux over 200-400 nm, is comparable to the Earth's. However, on Mars, the shorter wavelengths contribute a much



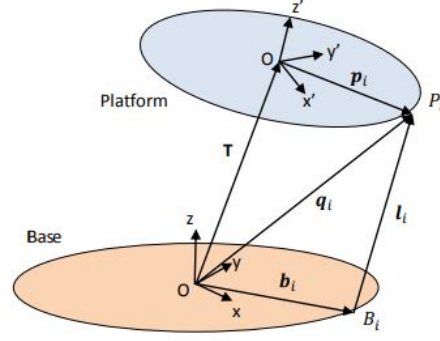


Figure 31: Coordinate system

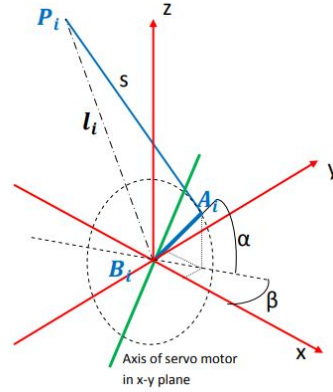


Figure 32: Spatial representation for each servo

greater proportion of this UV flux. These wavelength ranges are particularly biologically damaging. To tackle this Prepainted aluminum capable of withstanding the most severe weather conditions is used.

Low material outgassing is crucial for achieving and preserving extremely low pressures in the ultrahigh vacuum (UHV,  $p \leq 1 \cdot 10^{-7}$  mbar) and extremely high vacuum (XHV,  $p \leq 1 \cdot 10^{-11}$  mbar) region. Titanium alloy material has an excellent low outgassing property whose rate is lower than  $6 \times 10^{-13} [\text{U}+200\text{A}] \text{ Pa} [\text{U}+200\text{A}] \text{ m} [\text{U}+200\text{A}] \text{ s}^{-1}$ . [43]

### 11.4.3 Mathematics and Controls of Stewart Platform

The Stewart Platform consists of 2 rigid coordinate frames- Base with orthogonal coordinate frame x-y-z and Platform with  $x'-y'-z'$ . The platform has 6 degrees of freedom with respect to base frame- 3 translational and 3 angular. The full rotation matrix of the Platform relative to the Base is then given by:[44]

$${}^P R_B = R_z(\psi) \cdot R_y(\theta) \cdot R_x(\phi) \quad (18)$$

Now, consider  $i$  th leg of the Stewart Platform:

$$q_i = \mathbf{T} + {}^P R_B \cdot p_i \quad (19)$$



$$l_i = \mathbf{T} + {}^P R_{B.p_i} - b_i \quad (20)$$

$$\begin{aligned} l^2 - (s^2 - a^2) &= 2a \sin \alpha (z_p - z_b) + 2a \cos \alpha \cos \beta (x_p - x_b) + 2a \cos \alpha \sin \beta (y_p - y_b) \\ &= 2a \sin \alpha (z_p - z_b) + 2a \cos \alpha [\cos \beta (x_p - x_b) + \sin \beta (y_p - y_b)] \end{aligned} \quad (21)$$

variables as shown in figures. Now, consider

$$L = M \sin \alpha + N \cos \alpha$$

Using the Trig identity for the sum of sine waves

$$\begin{aligned} a \sin x + b \cos x &= c \sin(x + v) \\ \text{where } c &= \sqrt{a^2 + b^2} \quad \text{and} \quad \tan v = \frac{b}{a} \end{aligned}$$

We therefore have another sine function of  $\alpha$  with a phase shift  $\delta$

$$L = \sqrt{M^2 + N^2} \sin(\alpha + \delta) \quad \text{where} \quad \delta = \tan^{-1} \frac{N}{M}$$

Therefore

$$\sin(\alpha + \delta) = \frac{L}{\sqrt{M^2 + N^2}}$$

And

$$\begin{aligned} \alpha &= \sin^{-1} \frac{L}{\sqrt{M^2 + N^2}} - \tan^{-1} \frac{N}{M} \\ \text{where } L &= l^2 - (s^2 - a^2) \\ M &= 2a (z_p - z_b) \\ N &= 2a [\cos \beta (x_p - x_b) + \sin \beta (y_p - y_b)] \end{aligned}$$

#### 11.4.4 Working Principle of Spectrometry Analysis

When light passes through a medium, some part of the light is absorbed by the molecules of the medium. This absorption is governed by the laws of Beer[45]. The absorption of a solution is given by:

$$\text{Absorbance}(A) = \ln \frac{I_{\text{Incident}}}{I_{\text{Transmitted}}}$$

Whereas,  $I_{\text{Incident}}$  and  $I_{\text{Transmitted}}$  are the intensity of the incident and transmitted light through the solution.

We are measuring the intensity of the transmitted light with the help of a voltage divider network set up by an LDR and a fixed resistor. Different amount of light changes the voltage drop across the fixed resistor which we can measure using 16 bit analog to digital converter module. So, after the analog to digital conversion of the voltage drop across the fixed resistor, the representing number becomes an integer ranging from 0 to 32768 which is also proportional to the intensity of the light falling on the LDR[46]. After this point, we feed that value directly to equation 1 to get the absorbance value. Furthermore, the solution for which the absorbance will be measured, is also

prepared in this assembly. For example, quantification of protein will be done using this method in the following way:

- First the soil sample will be mixed with DI water then it will be filtered using the filtration systems.
- Then the filtered soil extract will be passed through a pump so that the flow of the solution does not depend on the gravity component in the testing environment.
- At higher fluid pressure, the solution will be passed into a mixing chamber where it is mixed with predefined amount of reagent. Then the mixture solution is passed into the spectrometer cuvette. This flow will be controlled by couple of solenoid valves placed on the fluid line.
- Then the internal cavity of the spectrometer will be full, light source will be turned on automatically to measure the voltage drop across the detector circuit (LDR+Resistor) when light falls on it after passing the solution.
- In colorimetric experiments, reference solution is used to represent the numerator part in equation 1. In our case we are getting the reference values by measuring voltage drop in the detector while passing the DI water without reagent through the fluid channels.
- The absorbance will be calculated and unknown concentration can be obtained by extrapolating calibration curves obtained before. The calibration curve will be plotted by measuring absorbance of solutions which will contain a known amount of protein.

### 11.4.5 Spectrometer Assembly Overview

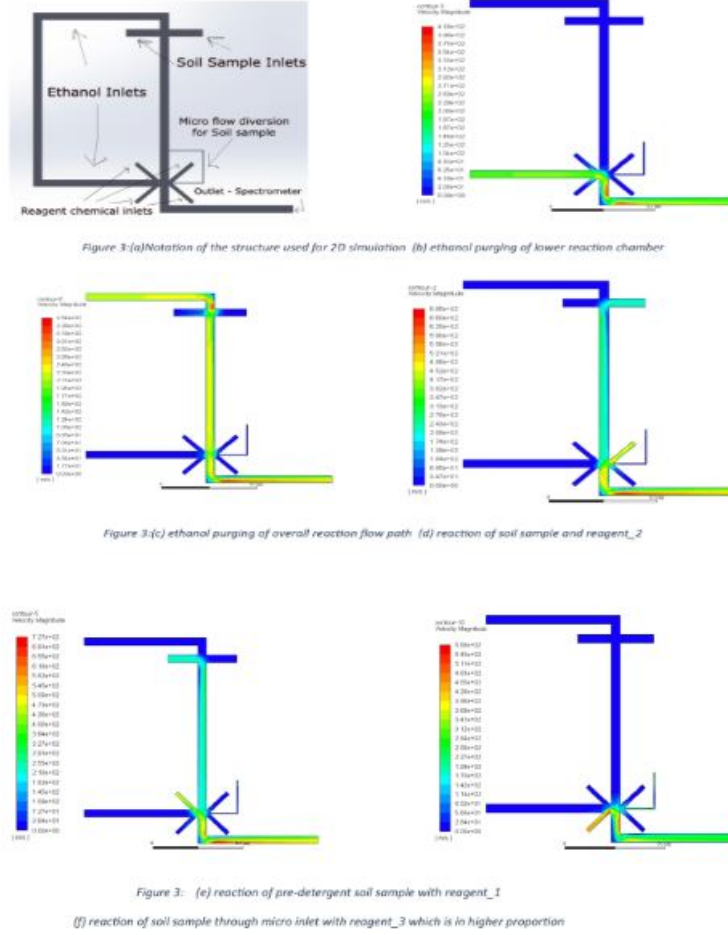


Figure 33: 2D CFD Simulation results

To achieve efficiency and capability to function in Martian condition, There are 3 Focus areas we concentrated on, that is 1) Chemical storage 2) electrical components 3) ambient conditions. Kapton Film Heaters are good thermal heating option for electric components which are motors, valves and pumps as explained before. For chemical storage chemical reservoirs are attached or connected to Heating conducting Tile on one of the face of Spectrometer Assembly Box. Which intakes heat from MMRTG based heat channel. Maintaining constant and high regulated ambient temperature is not required for Spectrophotometer and chemical reactions since chemicals and rest reaction chamber flow control points are already maintained at required heating level and whole experiment assembly is closed. Two dimensional CFD simulation results are shown in figure 33.

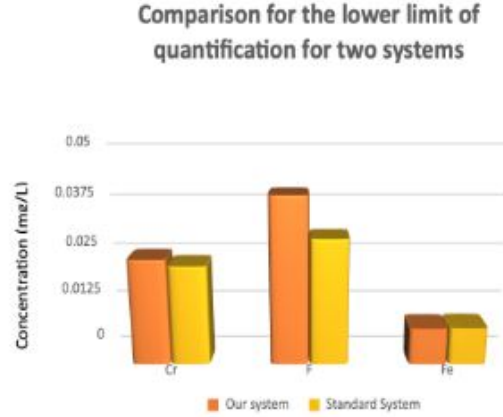


Figure 34: Comparison for the lower detection limit for the developed system and standard systems

To test the capabilities of the spectrometer, previously we tested multiple analytes and compared the results with market available standard spectrophotometric systems (Shimadzu UV 3600 spectrophotometer). 3 types of contaminants in drinking water (Iron, hexavalent chromium, fluoride). The comparison data is also represented in the figure 34. The lower limit of detection in those three cases does not differ from the values obtained from the standard systems for more than 3%. This test indicates that our detection and quantification process in the bio-assembly system can produce results without significant error.

## 11.5 Chassis

Important dimensions:

Part	Dimension
Chassis length	1400mm
Chassis breadth	1200mm
Chassis height	200mm
Square tube structural element dimension	20mmx20mmx2mm
Gusset plate thickness	10mm
Gusset side lengths	50mm, 50mm
Electrical box [lxbxh]	1160mmx600mmx160mm